Virology 486 (2015) 78–87

Contents lists available at ScienceDirect

Virology

journal homepage: www.elsevier.com/locate/yviro

FAITH – Fast Assembly Inhibitor Test for HIV

Romana Hadravová [a], Michaela Rumlová [a,b,*], Tomáš Ruml [c,**]

[a] Institute of Organic Chemistry and Biochemistry IOCB Research Centre & Gilead Sciences, Academy of Sciences of the Czech Republic, Flemingovo nám. 2, 166 10 Prague, Czech Republic
[b] Department of Biotechnology, University of Chemistry and Technology, Prague, Technická 5, 166 28 Prague, Czech Republic
[c] Department of Biochemistry and Microbiology, University of Chemistry and Technology, Prague, Technická 3, 166 28 Prague, Czech Republic

ARTICLE INFO

Article history:
Received 28 July 2015
Returned to author for revisions
25 August 2015
Accepted 27 August 2015
Available online 26 September 2015

Keywords:
Retrovirus
HIV
Assembly
Assay
Inhibitor
High-throughput screening
Capsid
CA

ABSTRACT

Due to the high number of drug-resistant HIV-1 mutants generated by highly active antiretroviral therapy (HAART), there is continuing demand for new types of inhibitors. Both the assembly of the Gag polyprotein into immature and mature HIV-1 particles are attractive candidates for the blocking of the retroviral life cycle. Currently, no therapeutically-used assembly inhibitor is available. One possible explanation is the lack of a reliable and simple assembly inhibitor screening method.

To identify compounds potentially inhibiting the formation of both types of HIV-1 particles, we developed a new fluorescent high-throughput screening assay. This assay is based on the quantification of the assembly efficiency *in vitro* in a 96-well plate format. The key components of the assay are HIV-1 Gag-derived proteins and a dual-labelled oligonucleotide, which emits fluorescence only when the assembly of retroviral particles is inhibited. The method was validated using three (CAI, BM2, PF74) reported assembly inhibitors.

Introduction

The current therapy for HIV-infected patients is mainly based on a combination of inhibitors of viral enzymes *i.e.* reverse transcriptase, protease and integrase or viral entry. Presently, 26 FDA approved anti-HIV drugs are available: seven nucleoside reverse transcriptase inhibitors (NRTIs), one nucleotide reverse transcriptase inhibitor (NtRTI), four non-nucleoside reverse transcriptase inhibitors (NNRTIs), 10 protease inhibitors (PIs), two integrase inhibitors (INIs), one fusion inhibitor, and one co-receptor inhibitor (De Clercq, 2010) (http://www.fda.gov). Despite the positive results from highly active antiretroviral therapy (HAART), there is continuing demand for new types of compounds that would help to overcome tolerance problems and more importantly, the emergence of high numbers of drug-resistant mutants generated by the error-prone reverse transcriptase and their selection in the presence of a particular inhibitor.

Similarly to other retroviruses, HIV-1 creates its infectious particles in two independent steps. In the first, the structural polyprotein Gag assembles at the plasma membrane and the resulting immature spherical particle buds from the cell. Viral protease is activated during the budding and cleaves the Gag polyprotein to yield MA, CA, and NC proteins that reassemble to form a mature, fully infectious virion. The MA protein remains associated with the viral envelope, while the mature CA assembles into a conical shell surrounding the condensed ribonucleoprotein complex of the NC protein and the viral RNA. Both the formation of the immature particle and the mature core are critical steps in the virus life cycle and the prevention of the interactions mediating these processes blocks the infectivity.

Although the virus assembly is an attractive candidate for inhibition, no suitable assembly inhibitor is currently available. Attempts to develop inhibitors interfering with the assembly yielded several compounds binding to CA, suggesting that CA may be a viable drug target. These compounds include: small-molecule inhibitors CAP-1 (Tang et al., 2003; Kelly et al., 2007), PF-74 (Blair et al., 2010), benzodiazepine derived compounds (BDs), benzimidazole derived compounds (BMs) (Lemke et al., 2012), and peptide inhibitor CAI (Sticht et al., 2005; Ternois et al., 2005). Another class of promising inhibitors are compounds blocking HIV maturation by inhibiting CA-SP1 cleavage, among them is PA-457 (bevirimat) (Li et al., 2003; Fujioka et al., 1994; Kanamoto et al., 2001; Zhou et al., 2004) and PF-46396 (Blair et al., 2009; Waki et al., 2012).

A number of studies have demonstrated that both assembly of an immature virus-like particle and a mature core can be performed *in vitro* from purified recombinant Gag-derived proteins

* Corresponding author at: UCT, Technická 3, 166 28 Prague, Czech Republic. Tel +420220444176.
** Corresponding author.
E-mail addresses: michaela.rumlova@vscht.cz (M. Rumlová), tomas.ruml@vscht.cz (T. Ruml).

http://dx.doi.org/10.1016/j.virol.2015.08.029

(Campbell and Vogt, 1995; Campbell and Rein, 1999; Ehrlich et al., 1992; Gross et al., 1997, 2000; Klikova et al., 1995; Rumlova-Klikova et al., 2000). HIV-1 Gag-derived proteins (*e.g.* CA and CANC) that assemble *in vitro* into narrow tubular and conical structures have a mature-like arrangement of CA (Campbell and Vogt, 1995; Ehrlich et al., 1992; Gross et al., 1997, 1998; Ganser et al., 1999; Li et al., 2000; von Schwedler et al., 1998; Bharat et al., 2014). In contrast, HIV-1 Gag derivatives known to assemble into spherical structures adopt an immature-like arrangement (Gross et al., 2000; von Schwedler et al., 1998; Bharat et al., 2014). The virus-like particle's *in vitro* assembly technique is a well-defined process based on the mixing of individual functional components (*i.e.* purified recombinant Gag-derived protein and an optional nucleic acid) and controlled adjustment of solvent conditions,

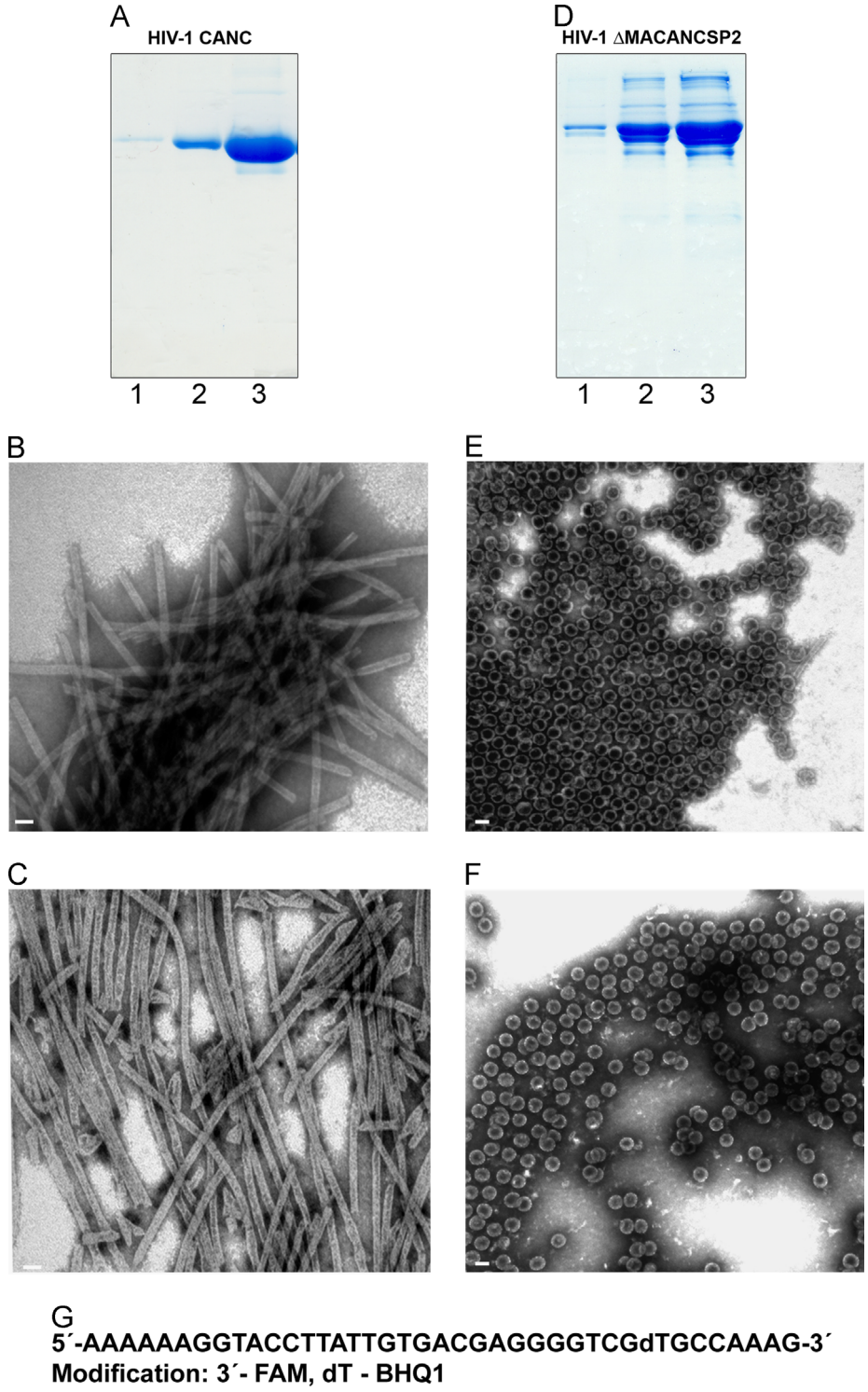

Fig. 1. *In vitro assembly of CANC (A–C) and ΔMACANCSP2 (D–F).* A, D: coomassie blue-stained SDS-polyacrylamide gel of purified (A) HIV-1 CANC: lane 1: 0.05 mg/ml, lane 2: 0.5 mg/ml, lane 3: 2.5 mg/ml; (D) ΔMACANCSP2: lane 1: 0.05 mg/ml, lane 2: 0.5 mg/ml, lane 3: 2.5 mg/ml. B–F: representative TEM images of negatively stained particles assembled *in vitro*: by dialysis against the assembly buffer containing 0.1 M NaCl: (B) CANC, (E) ΔMACANCSP2; by dilution to the assembly buffer containing 0.3 M NaCl (C) CANC, (F) ΔMACANCSP2; G. Sequence of tqON used for the *in vitro* assembly of HIV-1 CANC and ΔMACANCSP2. The tqON sequence is derived from the 3′ terminus of HIV-Gag and it is modified by FAM (at 3′ end) and BHQ1 at the eighth residue (designed dT) upstream from the 3′ end. Bar represents 100 nm.

usually by dialysis. The *in vitro* assembled material is then usually analyzed by electron microscopy. Apart from the cell-based assays quantifying the HIV-1 p24 antigen released from the infected cells exposed to tested compounds (Blair et al., 2009), several high-throughput screening assays based on the *in vitro* assembly of HIV-1 Gag derived proteins were published. Among them the turbidimetric assay for the quantitative monitoring of the rate of HIV-1 CA assembly and the immobilized capsid assembly assay (Lemke et al., 2012) have been described.

Here, we report the development of a *Fast Assembly Inhibitor Test for HIV* (*FAITH*). This method is based on the quantitation of assembly efficiency *in vitro* of both spherical and tubular HIV-1 particles formed from purified Gag-derived ΔMACANCSP2 and CANC proteins, respectively. The method was evaluated using inhibitors: CAI (Sticht et al., 2005), BM2 (Lemke et al., 2012), PF-074 (Blair et al., 2010), which were demonstrated to block retroviral assembly by targeting the different domains of Gag. The main advantages of our fluorescent method are i) it is a method for testing the assembly inhibitors in microtitre format solutions under physiological conditions; ii) it is sensitive, quantitative and fast; iii) it is simple and does not require any washing steps, and iv) it is not affected with DMSO up to final concentration of 1%.

Results

In vitro assembly of HIV-1 Gag-derived proteins by dilution

During its life cycle, HIV-1 subsequently assembles two types of particles, the immature and the mature one. It was shown that the interactions among the CA proteins, which stabilize the immature and mature viruses, are almost completely distinct (Bharat et al., 2012; Schur et al., 2015). HIV-1 Gag-derived proteins that assemble the spherical particles adopt immature-like arrays, while those assembled into tubular particles adopt a mature-like arrangement (Bharat et al., 2014). The *in vitro* assembly of the spherical particles was described for the Gag-derived protein lacking a p6 protein and amino acids 16-99 of the MA protein (ΔMACANCSP2) (Gross et al., 2000). The detailed cryo-EM study of the *in vitro* assembled spherical particles from the ΔMACANCSP2 protein revealed the same inner organization as that observed for the immature virions (Gross et al., 2000). The formation of mature-like tubular particles *in vitro* can be achieved using CA or CA-NC proteins (Campbell and Vogt, 1995; Ehrlich et al., 1992; Gross et al., 1997). The structural organization, in these tubular particles, resembles the arrangement observed in the mature conical cores (Li et al., 2000; Briggs et al., 2003). To increase the applicability of our assay on the assembly of both immature virus and mature core, we used two proteins: CANC for the formation of mature-like tubular particles and ΔMACANCSP2 for the formation of immature-like spherical particles (for the protein purity, see Fig. 1A and D, respectively).

The *in vitro* assembly of the retroviral particles is usually performed by mixing the stock solution of purified Gag-derived protein with an appropriate buffer, with optional nucleic acids, and by dialyzing this mixture against an assembly buffer (Campbell and Vogt, 1995; Gross et al., 1997; Klikova et al., 1995; Ulbrich et al., 2006). Since the dialysis step prevents a high-throughput screening, we used for the *in vitro* assembly a diluting method, in which we diluted the stock solution of either the CANC or ΔMACANCSP2 proteins into the assembly buffer containing oligonucleotides. To achieve the most effective *in vitro* assembly in the 96-well plate format, we optimized the conditions for the formation of both types of the particles. With an attempt to maximally mimic the physiological conditions, we focused on pH and ionic strength of the assembly buffer, on the protein to nucleic acid ratios and the size of the nucleic acid. The comparable yield of assembled structures to that obtained by the above mentioned dialysis method was achieved by dilution method using 18 μM CANC or 15 μM ΔMACANCSP2 at the protein to ON ratio at 10:1, at pH 8.0 in 300 mM NaCl (compare Fig. 1B, C and E, F). As neither the length nor the sequence of tested single-stranded DNA oligonucleotides significantly affected the efficiency of the dilution mediated assembly, the 40-meric sequence derived from the 3′ terminus of HIV-1 Gag was chosen (Fig. 1G). No assembled particles were observed by transmission electron microscopy in the control samples, containing only CANC or ΔMACANCSP2 proteins without the addition of the oligonucleotide (data not shown).

FAITH principle

The quantification of the assembly efficiency using FAITH is based on the use of a dual-labelled oligonucleotide (tqON). The tqON molecule is a single-stranded DNA oligonucleotide with a reporter dye-fluorescein (FAM) attached at its 3′ terminus and a quencher molecule-Black Hole Quencher (BHQ), which blocks the FAM fluorescence emission and it is attached to the eighth residue (designed dT) upstream from the 3′ end (Fig. 1G).

The *in vitro* assembly is triggered by the dilution of the stock solutions of purified CANC or ΔMACANCSP2 proteins to the assembly buffer and by the addition of tqON. During three-hour incubation, a certain amount of tqON is bound to the NC domain and packaged into the forming particles. Consequently, Exonuclease I (ExoI), that degrades tqON in a 3′→5′ direction, is added to the solution and the released fluorescence is measured. The tqON molecules wrapped in the assembled particles are protected by a protein shell against the ExoI cleavage. These intact tqON do not emit any fluorescence in contrast to the unprotected (unbound) portion of tqON, which is readily degraded by ExoI. The degradation of tqON results in the separation of the FAM quencher from the reporter BHQ molecule and subsequently to the increment of emitted fluorescence. The difference between fluorescence values of the control sample containing only free tqON and that consisting of CANC or ΔMACANCSP2 assembling in the presence of tqON is equivalent to the amount of protected tqON and expresses the efficiency of the assembly in the presence of tested inhibitor. The positive control represents co-assembly of either CANC or ΔMACANCSP2 with the tqON in the absence of inhibitor. Thus the ability of compounds to block the assembly of the immature or mature HIV-1 can be readily quantified based on the fluorescence released by the ExoI cleavage of the residual non-incorporated tqON.

The fluorescence recorded in a typical course of CANC and ΔMACANCSP2 assembly is shown in Fig. 2A and D, respectively. Here, the HIV-1 CANC or ΔMACANCSP2 proteins were diluted into the assembly buffer containing tqON in a 96-well plate. After 3-h incubation at room temperature, ExoI was added and the emitted fluorescence was continuously measured for 2 h by using a 96-well plate reader. The other essential control experiments without the tested inhibitors include i) a sample where only tqON in the absence of the retroviral protein is cleaved by ExoI, and ii) a sample where the retroviral protein is replaced with the assembly incompetent protein (BSA). As expected, no fluorescence was detected in CANC+tqON or ΔMACANCSP2+tqON containing samples without ExoI (Fig. 2A and D yellow curve). The addition of ExoI to the sample lacking the retroviral proteins led to degradation of free tqON resulting in the rapid increase of fluorescence (Fig. 2A and D red curve). The addition of ExoI to the same concentration of tqON in a presence of either CANC or ΔMACANCSP2 significantly reduced both the speed and the maximal yield of fluorescence emission (Fig. 2A and D blue curve) (compare Fig. 2A and D red and blue curves). The protection of tqON by assembled CANC or ΔMACANCSP2 is “protein specific” as documented by the

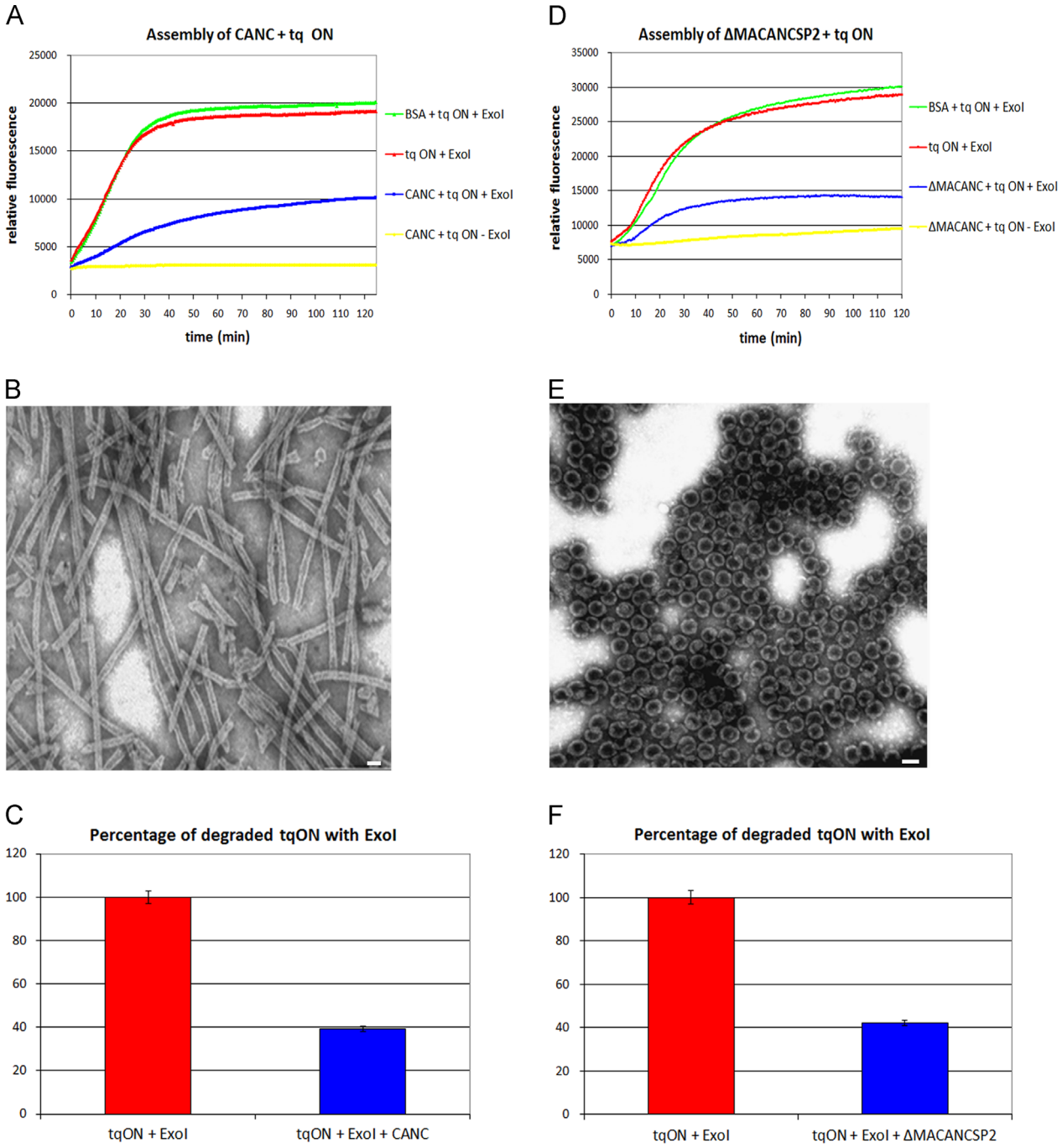

Fig. 2. *Quantification of in vitro assembly of HIV-1 CANC (A–C) and ΔMACANCSP2 (D–F) by FAITH.* Fluorescence emission curves demonstrating kinetics of degradation of tqON by ExoI in the controls and in the *in vitro* assembled (A) CANC and (D) ΔMACANCSP2 particles. ExoI catalysed degradation of tqON in the buffer (red curve) and in presence of BSA (green curve), ExoI catalysed degradation of tqON incorporated into either HIV-CANC (A) or ΔMACANCSP2 (D) (blue curve), control of stability of tqON incorporated into either HIV CANC (A) or ΔMACANCSP2 (D) in the absence of ExoI (yellow curve). B, E: TEM pictures of particles assembled in the presence of tqON and treated with ExoI CANC (B); ΔMACANCSP2 (E). Bars represent 100 nm. C, F: average percentage of degraded tqON in the buffer containing: tqON and ExoI (C, F red columns) and in the sample containing tqON, ExoI and either CANC or ΔMACANCSP2 (C or F blue columns, respectively).

negative control sample containing BSA+tqON (Fig. 2A and D green curve). The transmission electron microscopy (TEM) of negatively stained samples after fluorescence measurement correlated well with the FAITH results and confirmed the formation of tubular or spherical structures only in the samples containing CANC+tqON (Fig. 2B) or ΔMACANCSP2+tqON (Fig. 2E), respectively. TEM analysis of the control samples showed only protein precipitates (data not shown).

FAITH optimization and reproducibility

Quantification of the assembly efficiency in FAITH is based on efficient quantitative incorporation of tqON into the particles, which provides a sufficient difference of the nuclease triggered fluorescence signal between samples containing free tqON and tqON protected by the assembled protein shell. Therefore, we studied the effect of the protein to tqON ratio on the level of incorporated tqON. We found that the *in vitro* assembly occurs

within the range of protein:tqON wt:wt ratios from 10:0.1 to 10:2. The desired maximal incorporation of tqON into the CANC tubes or ΔMACANCSP2 spheres was obtained for both proteins at the protein:tqON (wt/wt] ratio of 10:0.5 (Fig. S1), which corresponds to molar ratios 7.5:1 and 8:1 for HIV CANC:tqON and ΔMACANCSP2:tqON, respectively. At this ratio, the incorporation of about 60% of the total tqON was achieved as measured within the interval 35–60 min, after the addition of 20 units of ExoI, at the protein concentration of 18 μM for CANC and 15 μM for ΔMACANCSP2 (*i.e.* 60 μg of protein and 3 μg of tqON in 100 μl reaction).

To validate the reproducibility of the presented method, the proteins were repeatedly expressed in independent cultivations and purified (CANC and ΔMACANCSP2 five and three times, respectively), and assembled in the presence of tqON from four independently-synthesized batches (Generi Biotech). Different batches of the ExoI enzyme (NEB, 3x) were tested as well. Results

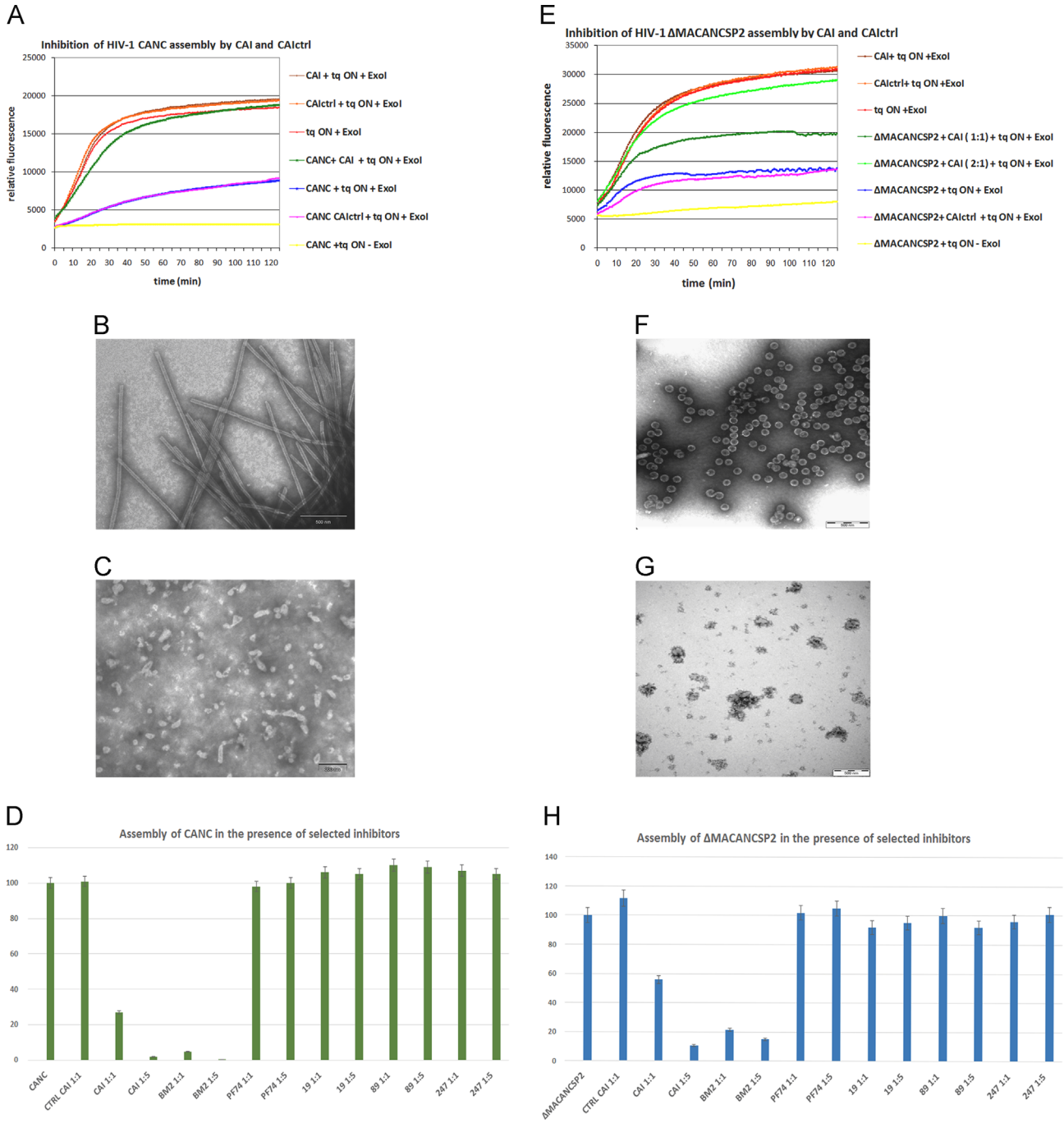

Fig. 3. *Quantification of in vitro assembly of HIV-1 CANC (A–D) and ΔMACANCSP2 (E–H) by FAITH in the presence of selected inhibitors.* Kinetic fluorescence emission curves of degradation of tqON by ExoI after the *in vitro* assembly of (A) CANC and (E) ΔMACANCSP2 in the presence of selected inhibitors. (3A, E): degradation of tqON in the presence of: CAI (brown curve), CAIctrl (orange curve), tqON only (red curve), (A) CANC or (E) ΔMACANCSP2 and CAI (green curve), (A) CANC or (E) ΔMACANCSP2 (blue curve), (A) CANC or (E) ΔMACANCSP2 CAIctrl (pink curve), and (A) CANC or (E) ΔMACANCSP2 without addition of ExoI (yellow curve). 3B, F: TEM pictures of the "pink curve" sample *i.e.* assembly of (B) CANC and (F) ΔMACANCSP2 in the presence of tqON and CAIctrl at the molar ratio protein:inhibitor 1:2. 3C, G: TEM pictures of the "green curve" sample *i.e.* assembly of (B) CANC and (F) ΔMACANCSP2 in the presence of tqON and CAI. 3D, H: percentage of efficiency of *in vitro* assembled (D) CANC or (H) ΔMACANCSP2 particles in the presence of selected inhibitors. Bar represents 100 nm.

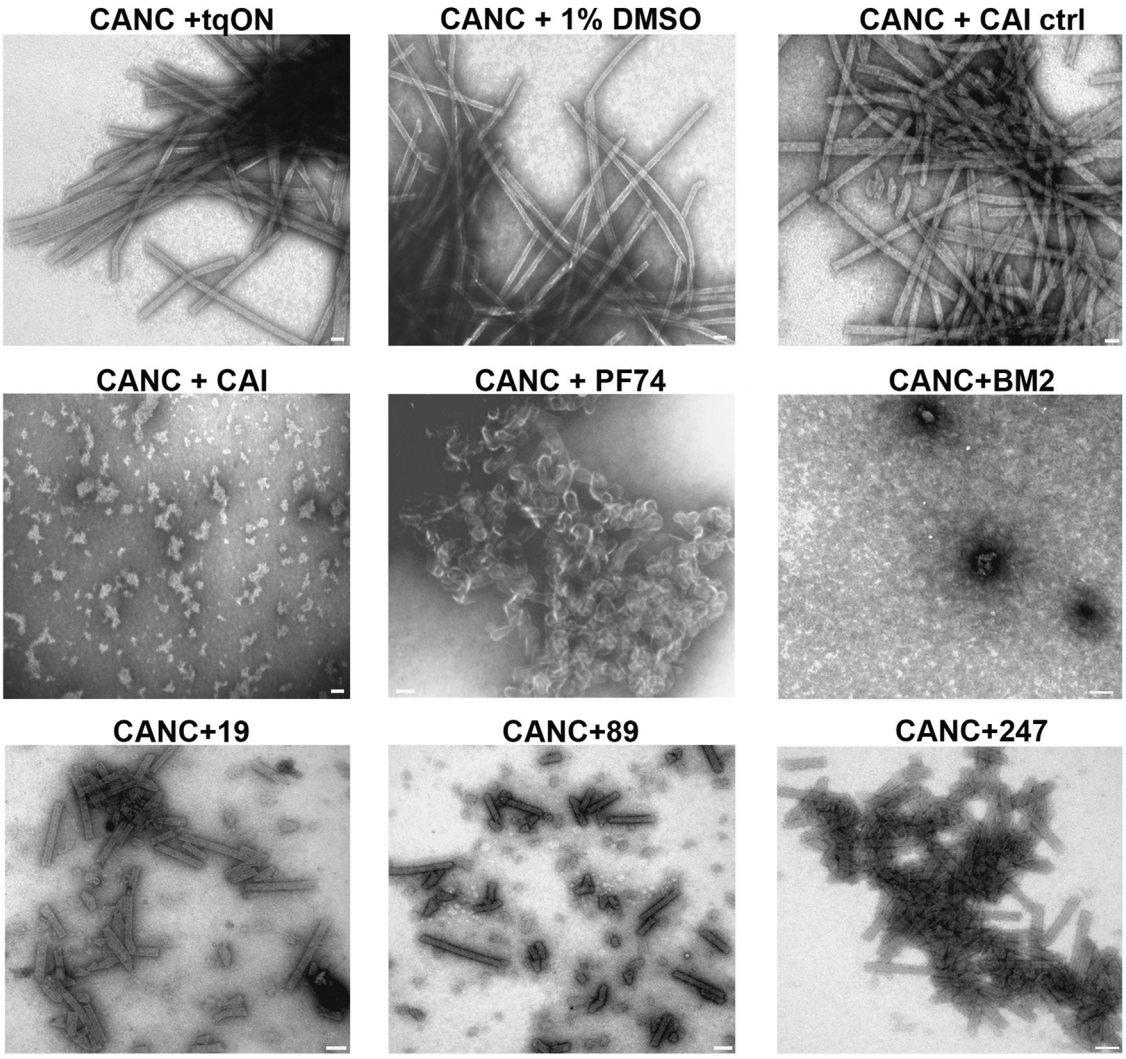

Fig. 4. *TEM analysis of assembled CANC particles in the presence of indicated inhibitors.* Following one-hour incubation of HIV CANC protein in the presence of indicated inhibitors or DMSO, the mixtures were diluted to the concentration optimal for assembly, tqON was added and the incubation proceeded for three-hours at RT. Then Exonuclease 1 and $MgCl_2$ were added and emitted fluorescence was measured by fluorescence reader. 10 μl aliquots of the reaction mixture were negatively stained with 2% phosphotungstic acid (pH 7.4) for 2×1 min, dried and visualized by using TEM. Bar represents 100 nm.

of these measurements were combined and are shown as a percentage of degraded tqON after the ExoI addition in the samples containing either tqON or tqON+CANC (Fig. 2C); tqON or tqON+ΔMACANCSP2 (Fig. 2F). The portion of residual tqON that remained protected by the CANC assemblage during ExoI cleavage was about 60% and in the case of ΔMACANCSP2, it was about 58%. The combined standard deviation of all these aforementioned experiments was less than 5% (Fig. 2C and F).

Validation of FAITH using known assembly inhibitors

The sensitivity of FAITH was validated using a CAI inhibitory peptide (ITFEDLLDYYGP) and its inactive derivative CAIctrl (IYDPTLYGLEFD), earlier published by Sticht et al. (2005). We performed the reaction in 96-well plate by mixing the CANC or ΔMACANCSP2 proteins with CAI or CAIctrl usually in an equimolar ratio. After 1 h incubation at 4 °C, the mixture was diluted in the assembly buffer containing the tqON and was incubated three hours. Then, the ExoI was added and the fluorescence was measured for $120 \times t$ 35 min. The level of inhibition was calculated as a percentage of the increased fluorescence ranging between controls represented with free tqON and that bound in the particles assembled in the absence of inhibitor. The efficiency of inhibitors was calculated from three independent measurements with three repetitions for each compound. Aliquots of the samples were negatively stained and analyzed by TEM.

The control measurements indicated that neither CAI nor CAIctrl affected the activity of ExoI as shown for the samples containing mere tqON (Fig. 3A and E red curves), tqON+CAI (Fig. 3A and E orange curves) and tqON+CAIctrl (Fig. 3A and E brown curves). As expected, the addition of the inactive inhibitor, CAIctrl to the CANC+tqON or ΔMACANCSP2+tqON samples did not affect the assembly as the emitted fluorescence time curve (Fig. 3A and E pink curves) almost copied those obtained for CANC+tqON and ΔMACANCSP2+tqON samples (Fig. 3A and E blue curves). In contrast, an equimolar concentration of CAI to the CANC+tqON sample (Fig. 3A green curve) efficiently inhibited the assembly resulting in a release of fluorescence signal similar to that of tqON alone. Unlike for CANC, the addition of CAI to ΔMACANCSP2+tqON sample in an equimolar ratio resulted in a lower increase of fluorescence (Fig. 3E dark green curve). However, more efficient inhibition was achieved with the molar ratio of protein to inhibitor of 1:5 (Fig. 3E light green curve). The inhibitory effect of the CAI peptide was further confirmed by TEM analyses. The efficient assembly of the CANC tubular particles was observed in the presence of the inactive CAIctrl (Fig. 3B) while only the free,

non-assembled protein was detected in the presence of the equimolar concentration of the active inhibitor CAI (Fig. 3C). Similarly, the inhibitory effect on the assembly of the ΔMACANCSP2 immature-like spherical particles was observed for CAI (Fig. 3G), but not for CAIctrl (Fig. 3F); both used at the molar ratio protein to inhibitor of 1:1 and 1:5.

To further evaluate the effectiveness of the FAITH, several inhibitors with different proposed modes of action were measured (Fig. 3D and H). We tested the derivatives of thioesters known to possess antiviral activity by zinc ejection from the NC zinc-binding domain labelled 19, 89 and 247 (Srivastava et al., 2004). Two other compounds, reported to block HIV-1 assembly were tested: PF3450074 (PF74) with the proposed effect both on assembly and uncoating of mature core (Blair et al., 2010; Lemke et al., 2012; Shi et al., 2011) and BM2, which upon binding, protrude from CANTD and prevent interactions with the neighbouring CACTD thus destabilizing the CANTD/CACTD interface in mature core (Blair et al., 2010; Lemke et al., 2012; Shi et al., 2011). The thioester derivatives had no effect on the assembly of both types of particles at a 1:1 or 1:5 ratios. The BM2 compound, at an equimolar (or higher) ratio, inhibited the HIV-1 mature particle, as well as the immature particle formation. However, the addition of PF74 affected the formation of neither the mature nor immature HIV-1 particles, which is consistent with the later published results, indicating that it rather than blocking the assembly, triggers premature uncoating in the target cells (Blair et al., 2010; Bhattacharya et al., 2014). Following fluorescence measurement, the samples were analyzed by TEM (Figs. 4 and 5).

Discussion

Despite the continuing need for new HIV inhibitors that would overcome the problem with emerging drug resistant strains, no FDA approved assembly inhibitor has yet been released. One of the reasons for this is very likely related to a methodical gap, *i.e.* the absence of an effective method for the screening of such compounds. In contrast, there is a broad spectrum of methods for enzymatic activity measurements available, and thus it is not surprising that the currently used anti-HIV drugs are inhibitors of reverse transcriptase, protease and integrase.

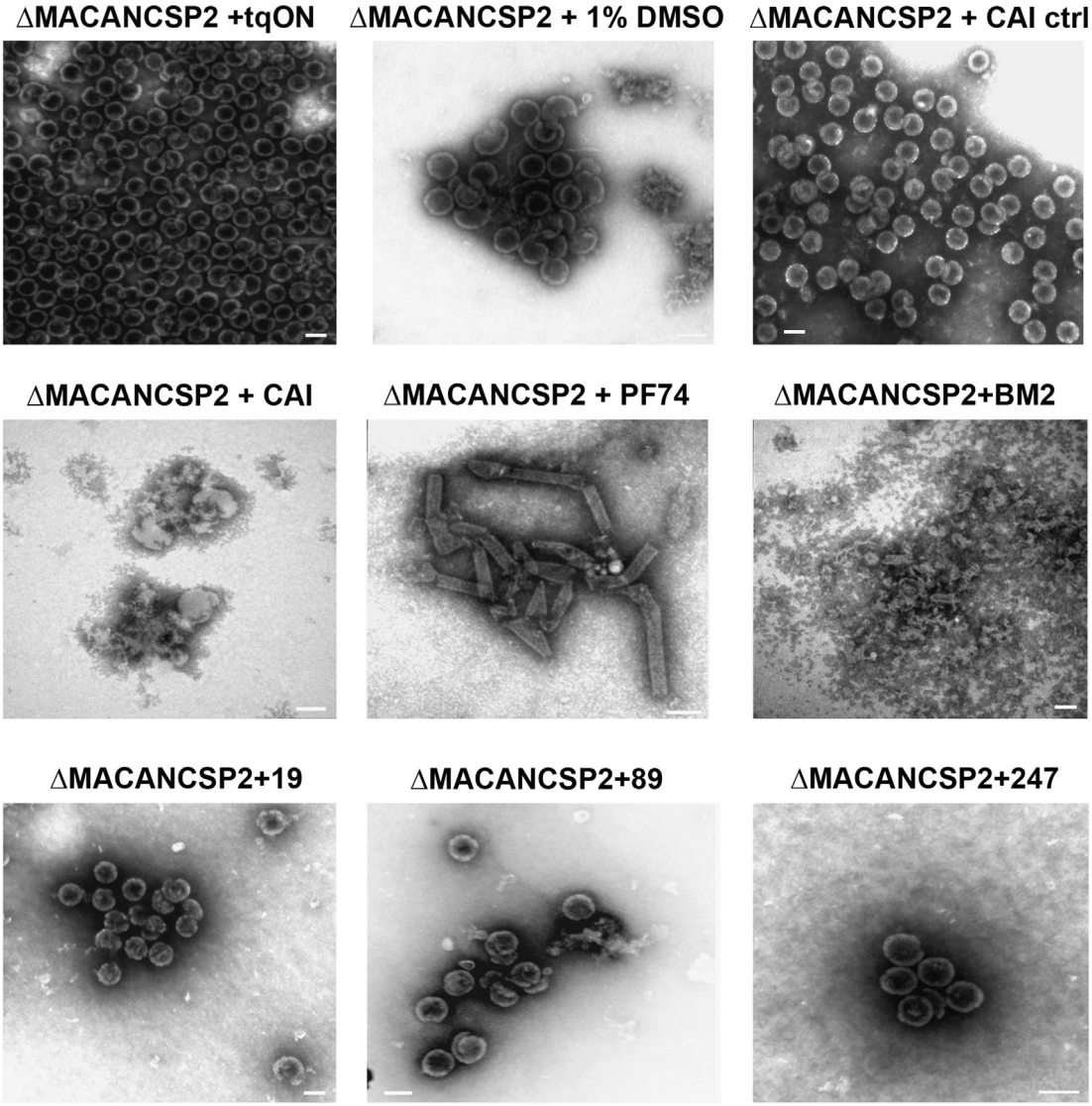

Fig. 5. *TEM analysis of assembled ΔMACANCSP2 particles in the presence of indicated inhibitors.* Following one-hour incubation of HIV ΔMACANCSP2 protein in the presence of indicated inhibitors or DMSO, the mixtures were diluted to the concentration optimal for assembly, tqON was added and the incubation proceeded for three-hours at RT. Then Exonuclease 1 and $MgCl_2$ were added and emitted fluorescence was measured by fluorescence reader. 10 μl aliquots of the reaction mixture were negatively stained with 2% phosphotungstic acid (pH 7.4) for 2 × 1 min, dried and visualized by using TEM. Bar represents 100 nm.

Lanman and Prevelige (2005) reported a method suitable for the high-throughput screening, which is based on monitoring the HIV-1 CA assembly kinetics by turbidity measurement. However, a high HIV-1 CA protein concentration (38-400 μM) and high NaCl concentration might affect protein interactions (1–2.25 M) and limit suitability of this method for screening under physiological conditions. Another high-throughput screening (HTS) method, using much lower protein and salt concentration, was reported by Lemke et al. (2012). This efficient HTS assay is based on the ability of NC to bind tightly to TG rich oligonucleotides, which are labelled by both biotin- and fluorescein. The biotin-labelled oligonucleotides are bound to the microplate surface and serve as a nucleation centre for CANC polymerization. The remaining unbound material is then washed away and the fluorescence is measured. The main drawback of the HTS assay is that mere interaction of the components, instead of the assembly might produce false positive results. Moreover, the polymerization of CANC on immobilized "scaffold-like" nucleic acid excludes direct confirmation of the assembled structures by EM. Also, the washing steps somehow complicate the HTS method.

The FAITH combines an improved protocol for the *in vitro* assembly with the usage of a dually labelled TaqMan-based oligonucleotide. We simplified the *in vitro* assembly of HIV-1 CA to a mere dilution of the protein from the stock solution to the assembly buffer in the presence of labelled oligonucleotide and subsequent addition of the exonuclease. The FAITH sensitivity is achieved by measurement of fluorescence signal released upon separating a single terminal nucleotide carrying the fluorescence label (FAM) from its quencher (BHQ). The principally fundamental difference of FAITH from the aforementioned methods is that the mere interaction of a protein with the nucleic acid is not sufficient for tqON protection against nucleases shown in the presence of CAI or BM2 inhibitors that both efficiently block the assembly but not the interaction of tqON with NC as indicated by an electrophoresis mobility shift assay (data not shown).

The model represented by CANC is distinct from the mature core assembled from mere CA and we are aware of such potential limitation. However, the fact that CANC assembles in tubular morphology and is sensitive to inhibitors of mature core assembly justifies its application as a model for a mature core consisting of both CA and NC with bound nucleic acid.

The published X-ray structure of the complex of the peptide inhibitor CAI with the HIV-1 CTD-CA shows that the α-helical CAI binds into the conserved hydrophobic groove of CTD-CA (formed by helices 1, 2 and 4), This interaction induces formation of a compact five helix bundle and alters dimeric interaction of CA-CTD (Ternois et al., 2005). In the *in vitro* assembly assays, it was shown that addition of an equimolar concentration of CAI to HIV-1 CANC protein efficiently abolished its assembly into tubular structures, whereas to prevent the assembly of immature particles, a five-fold molar excess of CAI was required (Sticht et al., 2005). We used CAI and its inactive control CAIctrl to validate our assay. Experimental data satisfactorily confirmed the fidelity of FAITH, as documented by the method itself as well as verified by TEM analysis the assembled particles (Figs. 4 and 5).

Apart from CAI peptide inhibitor, the TEM analysis confirmed also the activity of BM2 in blocking mature and immature assembly (Figs. 4 and 5). BH2 is one of the active benzimidazole compounds, shown to be a "bonafide" capsid assembly inhibitor binding to a pocket located at the base of the central four-helix bundle of the NTD-CA (Lemke et al., 2012). In order to verify whether this inhibitor of mature core assembly may bind also into immature CA lattice, an X-ray structure of a CA protein fragment complexed with one of the benzimidazole derived compounds BM4 (PDB ID: 4E92) was superimposed onto cryoEM-based structures of both immature and mature HIV-1 CA (PDB IDs: 4USN and 3J4F, respectively). Despite big differences in overall architecture of mature and immature CA lattices, the region defining the binding pocket of BM4 superimposes well with both types of lattices (data not shown). This can rationalize the fact that BM2 can bind to both types of lattices. Another inhibitor showing the expected FAITH results was PF74 inhibitor published to interfere with both the viral uncoating process and the formation of infectious particles (Blair et al., 2010). It did not abolish the *in vitro* assembly of either CANC (Fig. 4) or ΔMACANCSP2 (Fig. 5), which is consistent with the features of published co-crystal structure showing a novel binding pocket in the NTD-CA (Blair et al., 2010). This binding pocket between helices 3 and 4 is preformed in the hexamer and the binding PF74 to this site significantly increases the rate of CA assembly in *in vitro* studies (Blair et al., 2010; Bhattacharya et al., 2014). Interestingly, the presence of PF74 in the ΔMACANCSP2 assembly reaction affected structure of the particles and instead of spherical particles, a mixture of short rod-like or conical structures was observed (Fig. 5). It can be hypothesized, that binding of this compound shifted the equilibrium towards the conditions favoring mature-like assembly. It must be however noted that also the morphology of the mature-like CANC particles formed in the presence of PF74 differs from that assembled without the inhibitor (Fig. 4).

The results clearly demonstrate that the FAITH can be used for the testing of two types of HIV assembly inhibitors: i) those interfering with protein–protein interactions and ii) those blocking nucleic acid–protein interactions between tqON and NC. The advantage of this method is not only in its format, but also in its high sensitivity and simplicity as it is based on the pipetting of three solutions without any washing step.

Conclusions

The main advantages of the FAITH over the published methods are: i) the whole procedure is carried out under physiological conditions; ii) the assay's simplicity and nonobligatory washing steps, and iii) the assay is not affected by DMSO to a final concentration of 1%.

The high-throughput fluorescent method described here can broaden the opportunities for teams and companies searching for new types of viral inhibitors, *i.e.* those targeting the particle assembly or incorporation of a genomic nucleic acid.

Material and methods

Construct preparation

Preparation of expression vectors for HIV-1 CANC was described previously (Ulbrich et al., 2006). ΔMACANCSP2, encoding the deletion of 16-99 amino acid within MA, was constructed by inserting the *Cla*I-*Xho*I PCR fragment obtained from the pSAX2 vector (Rumlova et al., 2014) into the HIV-1 Δp6Gag pET expression vector. The whole HIV specific region was verified by sequence analysis.

Protein expression and purification

The HIV-1 CANC protein was purified as published previously (Campbell and Vogt, 1995; Ulbrich et al., 2006) with some modification. The HIV-1 CANC protein was expressed in *Escherichia coli* BL21 (DE3). The bacterial pellet (5 g) was resuspended in 25 ml of buffer D (20 mM Tris–HCl, pH 8, 0.5 M NaCl, 10% glycerol, 1 mM EDTA, 10 mM DTT, 1 mM Triton X-100, 1 mM PMSF) and the cells were disrupted by sonication (4 × 20 s) on ice. To the cell lysate,

polyethyleneimine to a final concentration 0.3% (w/v), was added and cell debris and nucleic acids were removed by ultracentrifugation (Beckman, TI 90, 55,000 rpm, 3 h, 4 °C). The HIV CANC protein was precipitated from the supernatant by ammonium sulphate (final concentration 25% (w/v)) at 4 °C. The precipitated protein was centrifuged (15,000 rpm, 15 min, 4 °C), resuspended in buffer E (20 mM Tris–HCl, pH 8.0, 0.1 M NaCl, 50 μM $ZnCl_2$, 10 mM DTT, 1 mM PMSF) and dialyzed overnight against the same buffer at 4 °C. The precipitate was removed by low speed centrifugation and the cleared supernatant was loaded on a DEAE cellulose column (bed volume 40 ml, flow rate 0.5 ml/min) in buffer E. The flow-through and washing fractions were pooled and loaded on the top of a phosphocellulose column (bed volume 50 ml, flow rate 0.5 ml/min). The bound proteins were eluted by a NaCl gradient from 0.1 M to 1 M NaCl in the buffer E. The fractions containing CANC protein were pooled and dialyzed overnight against a storage buffer (buffer E containing 0.5 M NaCl) at 4 °C. The proteins were concentrated to approximate volume of 5 ml and loaded on the top of Sephadex G-100 column (bed volume 470 ml, flow rate 0.1 ml/min) equilibrated in the buffer E with 0.5 M NaCl (storage buffer). The HIV CANC protein from pooled fractions were concentrated to 2–4 mg/ml and stored at −80 °C. The purity of the protein was analyzed by SDS-PAGE (Fig. 1 A). The expression/purification process of ΔMACANCSP2 protein was similar as that described above, only the step of polyethylenimine and ammonium sulphate precipitation was omitted. The purity of the protein was analyzed by SDS-PAGE (Fig. 1D).

In vitro assembly by dialysis

An aliquot of 60 μg of purified HIV CANC or ΔMACANCSP2 protein was mixed with 40-mer oligonucleotide ON or FAM-BHQ modified ON (tqON) (Fig. 1G) in a final protein: oligonucleotide 10:0.5 (wt/wt) ratio, which corresponds to molar ratios 7.5:1 and 8:1 for HIV CANC:tqON and ΔMACANCSP2:tqON, respectively. The final reaction volume was adjusted to 100 μl by the storage buffer (20 mM Tris–HCl, pH 8.0, 0.5 M NaCl, 50 μM $ZnCl_2$, 10 mM DTT, 1 mM PMSF) and the mixture was dialyzed against the assembly buffer (50 mM Tris–HCl, pH 8.0, 100 mM NaCl, 1 μM $ZnCl_2$) for 3 h at room temperature. The dialysate was used for TEM.

In vitro assembly by dilution

Purified HIV-1 CANC or ΔMACANCSP2 protein in the storage buffer (20 mM Tris–HCl, pH 8.0, 0.5 M NaCl, 50 μM $ZnCl_2$, 10 mM DTT, 1 mM PMSF) was rapidly diluted by the assembly buffer (50 mM Tris–HCl, pH 8.0, 100 mM NaCl, 1 μM $ZnCl_2$) in 96-well plate format so that the final concentration of NaCl was 300 mM, CANC protein 18 μM (60 μg/100 μl) and ΔMACANCSP2 protein 15 μM (60 μg/100 μl). Immediately after the dilution, the 40-mer oligonucleotide ON or FAM-BHQ modified ON (tqON) was added (Fig. 1G) at the final protein:ON ratio usually 10:0.5 in a final sample volume of 100 μl and was incubated 3 h at room temperature. The samples were used for TEM.

Inhibition of in vitro assembly

The inhibitor was added to the HIV CANC or ΔMACANCSP2 protein in the storage buffer (20 mM Tris–HCl, pH 8.0, 0.5 M NaCl, 50 μM $ZnCl_2$, 10 mM DTT, 1 mM PMSF) typically in the final molar ratio protein:inhibitor 1:1, 1:2 or 1:5, and the mixture was incubated for 1 h on ice. Then the mixture was rapidly diluted with the assembly buffer (50 mM Tris–HCl, pH 8.0, 100 mM NaCl, 1 μM $ZnCl_2$) so that the final concentration of NaCl was 0.3 M, CANC protein 18 μM (60 μg/100 μl), ΔMACANCSP2 protein 15 μM (60 μg/100 μl) and the procedure continued as described above. Optionally, if the inhibitor was solubilized in DMSO, the final concentration of DMSO was up to 1%.

Fluorescence measurement

Following the one-hour incubation of HIV CANC and ΔMACANCSP2 protein in the presence of inhibitor (as described above), the mixtures were diluted a final sample volume of 100 μl by the assembly buffer (50 mM Tris–HCl, pH 8.0, 100 mM NaCl, 1 μM $ZnCl_2$) to a final concentration of NaCl 0.3 M, CANC protein 18 μM (60 μg/100 μl), and ΔMACANCSP2 protein 15 μM (60 μg/100 μl), DMSO up to 1%, tqON was added and the incubation proceeded for three-hour at RT. To the 100 μl of reaction mixtures in the 96-well plate, 20 U/μl of Exonuclease 1 (NEB) and $MgCl_2$, to a final concentration of 6.7 mM, were added and emitted fluorescence was immediately measured by fluorescent reader (Tecan Infinite M1000) for 120 min. The excitation and emission wavelengths corresponded to 495 nm and 520 nm, respectively.

Electron microscopy

Particles formed during assembly reaction were visualized by negative staining. Parlodion-carbon-coated grids were floated on the top of 5 ul drop of the sample, washed in distilled water and transferred on the top of drop 2% phosphotungstic acid (pH 7.4), stained for 2 × 1 min and dried. Photomicrographs were taken with a JEOL JEM-1200EX electron microscope operated at 60 kV.

Authors' contributions

RH performed cloning, proteins purification, *in vitro* assembly assay, fluorescence measurement, and EM, MR conceived the ideas, designed the experiments, and prepared the manuscript, TR conceived the ideas and contributed to manuscript preparation.

Acknowledgments

We thank Romana Cubínková for excellent technical assistance and Thea Baum for language correction. We are also grateful to Dr. Vojtech Spiwok (UCT, Prague) for *in silico* modelling of the complexes of BM4 with immature and mature HIV-1 CA structures, Prof. Alex McPherson from University of California Irvine for valuable suggestions and Dr. Appella from NCI, USA for providing us with thioester derivatives (19, 89 and 247) and Dr. Tomáš Cihlář from Gilead for providing us with BM2 and PF74 compounds. This work was supported by the Grant Agency of the Czech Republic Grant number 14-15326S to MR and by NPU I Projects LO 1302 and LO 1304 and LN12011 from Ministry of Education.

Appendix A. Supplementary material

Supplementary data associated with this article can be found in the online version at http://dx.doi.org/10.1016/j.virol.2015.08.029.

References

Blair, W.S., Pickford, C., Irving, S.L., Brown, D.G., Anderson, M., Bazin, R., Cao, J., Ciaramella, G., Isaacson, J., Jackson, L., Hunt, R., Kjerrstrom, A., Nieman, J.A., Patick, A.K., Perros, M., Scott, A.D., Whitby, K., Wu, H., Butler, S.L., 2010. PLoS Pathog. 6, e1001220.

Blair, W.S., Cao, J., Fok-Seang, J., Griffin, P., Isaacson, J., Jackson, R.L., Murray, E., Patick, A.K., Peng, Q., Perros, M., Pickford, C., Wu, H., Butler, S.L., 2009. Antimicrob. Agents Chemother. 53, 5080–5087.

Bharat, T.A.M., Castillo Menendez, L.R., Hagen, W.J.H., Lux, V., Igonet, S., Schorb, M., Schur, F.K.M., Kräusslich, H.-G., Briggs, J.A.G., 111 2014. Proc. Natl. Acad. Sci. USA 111, 8233–8238.
Bharat, T.A., Davey, N.E., Ulbrich, P., Riches, J.D., de, M.A., Rumlova, M., Sachse, C., Ruml, T., Briggs, J.A., 2012. Nature 487, 385–389.
Briggs, J.A., Wilk, T., Welker, R., Krausslich, H.G., Fuller, S.D., 2003. EMBO J. 22, 1707–1715.
Bhattacharya, A., Alam, S.L., Fricke, T., Zadrozny, K., Sedzicki, J., Taylor, A.B., Demeler, B., Pornillos, O., Ganser-Pornillos, B.K., Diaz-Griffero, F., Ivanov, D.N., Yeager, M., 2014. Proc. Natl. Acad. Sci. USA 111, 18625–18630.
Campbell, S., Vogt, V.M., 1995. J. Virol. 69, 6487–6497.
Campbell, S., Rein, A., 1999. J. Virol. 73, 2270–2279.
De Clercq, E., 2010. Future Med. Chem. 2, 1049–1053.
Ehrlich, L.S., Agresta, B.E., Carter, C.A., 1992. J. Virol. 66, 4874–4883.
Fujioka, T., Kashiwada, Y., Kilkuskie, R.E., Cosentino, L.M., Ballas, L.M., Jiang, J.B., Janzen, W.P., Chen, I.S., Lee, K.H., 1994. J. Nat. Prod. 57, 243–247.
Gross, I., Hohenberg, H., Krausslich, H.G., 1997. Eur. J. Biochem. 249, 592–600.
Gross, I., Hohenberg, H., Wilk, T., Wiegers, K., Grattinger, M., Muller, B., Fuller, S., Krausslich, H.G., 2000. EMBO J. 19, 103–113.
Ganser, B.K., Li, S., Klishko, V.Y., Finch, J.T., Sundquist, W.I., 1999. Science 283, 80–83.
Gross, I., Hohenberg, H., Huckhagel, C., Krausslich, H.G., 1998. J. Virol. 72, 4798–4810.
Kelly, B.N., Kyere, S., Kinde, I., Tang, C., Howard, B.R., Robinson, H., Sundquist, W.I., Summers, M.F., Hill, C.P., 2007. J. Mol. Biol. 373, 355–366.
Kanamoto, T., Kashiwada, Y., Kanbara, K., Gotoh, K., Yoshimori, M., Goto, T., Sano, K., Nakashima, H., 2001. Antimicrob. Agents Chemother. 45, 1225–1230.
Klikova, M., Rhee, S.S., Hunter, E., Ruml, T., 1995. J. Virol. 69, 1093–1098.
Lemke, C.T., Titolo, S., von Schwedler, U., Goudreau, N., Mercier, J.F., Wardrop, E., Faucher, A.M., Coulombe, R., Banik, S.S., Fader, L., Gagnon, A., Kawai, S.H., Rancourt, J., Tremblay, M., Yoakim, C., Simoneau, B., Archambault, J., Sundquist, W.I., Mason, S.W., 2012. J. Virol. 86, 6643–6655.
Li, F., Goila-Gaur, R., Salzwedel, K., Kilgore, N.R., Reddick, M., Matallana, C., Castillo, A., Zoumplis, D., Martin, D.E., Orenstein, J.M., Allaway, G.P., Freed, E.O., Wild, C. T., 2003. Proc. Natl. Acad. Sci. USA 100, 13555–13560.
Li, S., Hill, C.P., Sundquist, W.I., Finch, J.T., 2000. Nature 407, 409–413.
Lanman, J., Prevelige Jr., P.E., 2005. Adv. Virus Res. 64, 285–309.
Rumlova-Klikova, M., Hunter, E., Nermut, M.V., Pichova, I., Ruml, T., 2000. J. Virol. 74, 8452–8459.
Rumlova, M., Krizova, I., Keprova, A., Hadravova, R., Dolezal, M., Strohalmova, K., Pichova, I., Hajek, M., Ruml, T., 2014. Retrovirology 11, 37.
Sticht, J., Humbert, M., Findlow, S., Bodem, J., Muller, B., Dietrich, U., Werner, J., Krausslich, H.G., 2005. Nat. Struct. Mol. Biol. 12, 671–677.
Schur, F.K., Hagen, W.J., Rumlova, M., Ruml, T., Muller, B., Krausslich, H.G., Briggs, J. A., 2015. Nature 517, 505–508.
Srivastava, P., Schito, M., Fattah, R.J., Hara, T., Hartman, T., Buckheit Jr., R.W., Turpin, J.A., Inman, J.K., Appella, E., 2004. Bioorg. Med. Chem. 12, 6437–6450.
Shi, J., Zhou, J., Shah, V.B., Aiken, C., Whitby, K., 2011. J. Virol. 85, 542–549.
Tang, C., Loeliger, E., Kinde, I., Kyere, S., Mayo, K., Barklis, E., Sun, Y., Huang, M., Summers, M.F., 2003. J. Mol. Biol. 327, 1013–1020.
Ternois, F., Sticht, J., Duquerroy, S., Krausslich, H.G., Rey, F.A., 2005. Nat. Struct. Mol. Biol. 12, 678–682.
Ulbrich, P., Haubova, S., Nermut, M.V., Hunter, E., Rumlova, M., Ruml, T., 2006. J. Virol. 80, 7089–7099.
Waki, K., Durell, S.R., Soheilian, F., Nagashima, K., Butler, S.L., Freed, E.O., 2012. PLoS Pathog. 8, e1002997.
Zhou, J., Yuan, X., Dismuke, D., Forshey, B.M., Lundquist, C., Lee, K.H., Aiken, C., Chen, C.H., 2004. J. Virol. 78, 922–929.
von Schwedler, U.K., Stemmler, T.L., Klishko, V.Y., Li, S., Albertine, K.H., Davis, D.R., Sundquist, W.I., 1998. EMBO J. 19, 2391 2391.